Mon. Not. R. Astron. Soc. **333,** 27–38 (2002)

The type IIn supernova 1995G: interaction with the circumstellar medium

A. Pastorello,[1★] M. Turatto,[2] S. Benetti,[2] E. Cappellaro,[2] I. J. Danziger,[4] P. A. Mazzali,[3] F. Patat,[5] A. V. Filippenko,[6] D. J. Schlegel[6]† and T. Matheson[6]‡

[1]*Dipartimento di Astronomia, Università di Padova, vicolo dell'Osservatorio 2, 35122 Padova, Italy*
[2]*Osservatorio Astronomico di Padova, vicolo dell'Osservatorio 5, 35122 Padova, Italy*
[3]*Osservatorio Astronomico di Capodimonte, via Moiariello 16, 80131 Napoli, Italy*
[4]*Osservatorio Astronomico di Trieste, via G.B. Tiepolo 11, 34131 Trieste, Italy*
[5]*European Southern Observatory, Karl Schwarzschild-Strasse 2, D-85748, Garching bei München, Germany*
[6]*Department of Astronomy, University of California, Berkeley, CA 94720–3411, USA*

Accepted 2002 January 23. Received 2001 December 20; in original form 2001 September 27

ABSTRACT

We present the photometric and spectroscopic evolution of the type IIn SN 1995G in NGC 1643, on the basis of 4 years of optical and infrared observations. This supernova shows very flat optical light curves similar to SN 1988Z, with a slow decline rate at all times. The spectra are characterized by strong Balmer lines with multiple components in emission and with a P Cygni absorption component blueshifted by only 700 km s^{-1}. This feature indicates the presence of a slowly expanding shell above the SN ejecta as in the case of SNe 1994aj and 1996L. As in other SNe IIn, the slow luminosity decline cannot be explained only with a radioactive energy input, and an additional source of energy is required, most likely that produced by the interaction between supernova ejecta and a pre-existent circumstellar medium (CSM). It was estimated that the shell material has a density $n_{\rm H} \gg 10^8$ cm^{-3}, consistent with the absence of forbidden lines in the spectra. About 2 years after the burst the low-velocity shell is largely overtaken by the SN ejecta and the luminosity drops at a faster rate.

Key words: circumstellar matter – supernovae: general – supernovae: individual: SN 1995G – supernovae: individual: SN 1988Z – galaxies: individual: NGC 1643.

1 INTRODUCTION

Supernovae of type II (SNe II) are characterized by H lines in their spectra. Among them a subclass has been isolated which shows slow photometric evolution, absence of broad P Cygni absorptions, and emission lines (Hα, in particular) with multiple components. Schlegel (1990) labelled these SNe as type IIn, where the 'n' stands for 'narrow', although this designation is somewhat misleading because of the simultaneous presence of narrow and broad components. Best-studied cases of this class are SN 1988Z (Stathakis & Sadler 1991; Turatto et al. 1993; Filippenko 1997; Aretxaga et al. 1999) and SN 1995N (Fox et al. 2000; Fransson et al. 2001). We recall that some very bright SNe IIn with very broad emission components, implying velocities as large as 17 000 km s^{-1}, may be associated with GRB, namely SN 1997cy (Turatto et al. 2000) and SN 1999E (Cappellaro, Turatto & Mazzali 1999; Filippenko, Leonard & Riess 1999). Another group, sometimes called SNe IId (or SNe IIsw), shows narrow P Cygni absorptions on top of otherwise normal SNe II spectra [SN 1984E (Dopita et al. 1984), SN 1994aj (Benetti et al. 1998), SN 1996L (Benetti et al. 1999) and SN 1996al (Benetti et al. in preparation)]. These features have been explained by the presence of a thick expanding shell above the photosphere.

The present paper contains an extensive study of SN 1995G, an object which, sharing properties both of SN 1988Z and SNe IId, reinforces the link between these apparently different objects. It is worth recalling that a few other objects sharing some of the features of SN 1995G have been reported in recent years, i.e., SN 1997ab (Salamanca et al. 1998), SN 1997eg (Salamanca, Terlevich & Tenorio-Tagle 2002) and SN 1998S (Fassia et al. 2000, 2001).

SN 1995G was discovered by Evans et al. (1995) on Feb. 23.5 U.T., using the 1-m reflector of the Australian National University in Siding Spring at an apparent visual magnitude of 15.5. McNaught & Cass (1995) measured the SN position as RA = $04^{\rm h}43^{\rm m}44\overset{\rm s}{.}22$, Dec. = $-05°18'53\overset{''}{.}8$ (equinox 2000.0), 4.5 arcsec east and 16.1 arcsec north from the centre of NGC 1643 (see Fig. 1), an Sbc galaxy, with $v_{\rm helio} = 4850 \pm 29$ km s^{-1} (Huchra et al. 1993). Lacking other determinations, in the

★E-mail: pastorello@pd.astro.it
†Present address: Department of Astrophysical Sciences, Peyton Hall, Princeton University, Princeton, NJ 08544, USA.
‡Present address: Center for Astrophysics, 60 Garden Street, Cambridge, MA 02138, USA.

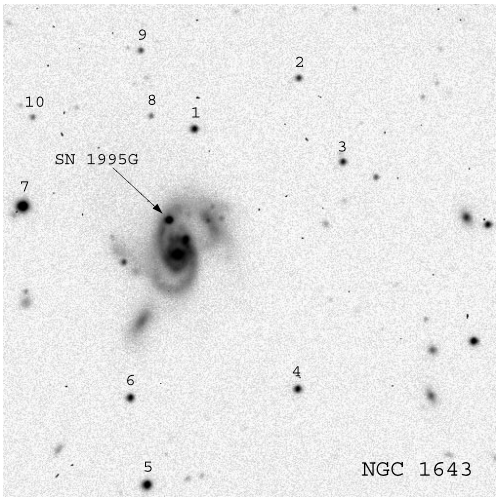

Figure 1. Identification of SN 1995G and the stars of the local sequence around NGC 1643 (see Table 2). North is up, and east is to the left.

Table 1. Main data on SN 1995G and the host galaxy.

SN 1995G		
α (J2000.0)	$04^{h}43^{m}44^{s}.22$	$\diamond$
δ (J2000.0)	$-05°18'53''.8$	$\diamond$
Offset SN - Gal. Nucleus	4″.5E, 16″.1N	$\diamond$
SN Type	IIn	$\otimes$
Discovery Date	1995 Feb 23.5	$\odot$
(Julian Date)	(2449772)	$\odot$
Discovery Magnitude	15.5	$\odot$
NGC 1643		
α (J2000.0)	$04^{h}43^{m}44^{s}$	$\star$
δ (J2000.0)	$-05°19'10''$	$\star$
Morph. Type	SB(r)bc pec?	$\star$
Magnitude	14.00	$\triangle$
Galactic Extinction A_B	0.19	$\star$
Diameters	$1'.0 \times 1'.0$	$\triangle$
$v_{\rm helio}$ (km s^{-1})	4850 ± 29	$\triangle$
μ ($H_0 = 65$ km s^{-1} Mpc^{-1})	34.32	†

$\diamond$ (McNaught & Cass 1995).
$\otimes$ (Filippenko & Schlegel 1995).
$\star$ (de Vaucouleurs et al. 1991).
$\odot$ (Evans et al. 1995).
$\triangle$ (Huchra et al. 1993).
† LEDA.

following we will adopt the galaxy distance modulus derived from the recession velocity, after correction for the Local Group infall into the Virgo Cluster (LEDA[1]). Assuming $H_0 = 65$ km s^{-1} Mpc^{-1}, we obtain $\mu = 34.32$ (cf. Section 4.2).

The basic information on SN 1995G and the parent galaxy is summarized in Table 1. It is worth mentioning that another type II supernova, SN 1999et (Cappellaro 1999), has been discovered in the same host galaxy.

We checked that no γ-ray burst has been detected by BATSE in the months before the discovery within 2 error radii from the position of SN 1995G. The closest event is burst 4B 950206B, which occurred 18 days before SN 1995G discovery at 2.33 BATSE error radii.

The observations of SN 1995G, described in Section 2, are analysed in Sections 3 and 4. The discussion of the data is given in Section 5, and the conclusions are summarized in Section 6.

[1] http://leda.univ-lyon1.fr

2 OBSERVATIONS

The photometric observations of SN 1995G in the optical bands cover a period of about 2.5 years. They were carried out using various ESO telescopes at La Silla and the Asiago 1.82-m reflector.

CCD frames were reduced in the IRAF environment, applying bias and flat-field corrections. At early phases, when the SN was bright, the SN magnitudes were measured with a PSF-fitting technique, which was preferred over aperture photometry because of the location of the SN inside a spiral arm. The late time photometry was obtained by means of a template subtraction technique, i.e., subtracting from the frame to be measured a late (5 years after discovery) image of the field after proper geometric, photometric and PSF matching.

The SN photometry has been performed relative to a local sequence (Fig. 1), calibrated during several photometric nights by comparison with standard stars from the list of Landolt (1992). The magnitudes of the local sequence and those of the SN are reported in Tables 2 and 3, respectively. At the last epochs since the SN was not detected, only upper limits are reported.

Errors on the magnitudes of the local-sequence stars are estimated as the rms of the available measurements (no error is reported if only one measure is available). Photometric errors of the SN were estimated for some representative epochs (col. 6 of Table 3). They have been obtained via artificial star experiments, placing stars of the same magnitude as that of the SN in locations close to that of the SN, and then computing the deviations of the recovered magnitudes.

In addition to optical data, a number of late infrared observations have been obtained. For each epoch, a sequence of SN and nearby sky frames are available. After flat-field correction and sky subtraction, the frames were aligned and combined. For the IR photometric calibration we used standard stars taken from Carter & Meadows (1995), Hunt et al. (1998) and Persson et al. (1998). The local sequence consists of only two stars in the field (see Fig. 2 and Table 4). The IR magnitudes of SN 1995G are reported in Table 3. Typical errors of the SN infrared magnitudes are 0.2 mag (0.4 mag on 1997 September 17).

Optical spectroscopic observations were obtained at La Silla, Asiago and Lick Observatories. The log of these observations is given in Table 6. Wavelength calibrations were performed using comparison spectra of HeAr lamps, while the flux calibration was done using spectra of standard stars (Stone & Baldwin 1983; Baldwin & Stone 1984; Hamuy et al. 1992, 1994) taken during the same nights. We made also an attempt to correct the SN spectra for atmospheric absorption lines by comparison with the observed spectrum of a featureless hot star. Finally, the flux calibration of the reduced SN spectra was checked against the broad-band photometry, and found to be in reasonable agreement (a typical error is ± 20–30 per cent).

3 PHOTOMETRY

3.1 Optical light and colour curves

The *BVRI* light curves of SN 1995G (plus two measurements in *U*) are shown in Fig. 3. Though there are not definite evidences, we believe that the SN was discovered very close to maximum

Table 2. Magnitudes of the local sequence as identified in Fig. 1.

	1	2	3	4	5
U	18.26 ± 0.09	18.74	18.83 ± 0.04	18.53 ± 0.13	17.37 ± 0.08
B	18.11 ± 0.02	18.95 ± 0.02	18.65 ± 0.02	18.19 ± 0.02	17.08 ± 0.02
V	17.36 ± 0.01	18.36 ± 0.02	17.94 ± 0.02	17.42 ± 0.01	16.31 ± 0.01
R	16.89 ± 0.01	18.01 ± 0.01	17.46 ± 0.02	16.95 ± 0.01	15.81 ± 0.01
I	16.47 ± 0.01	17.68 ± 0.01	17.08 ± 0.02	16.52 ± 0.01	15.38 ± 0.03
	6	7	8	9	10
U	17.97 ± 0.03	16.21	19.54	20.00	20.03
B	17.99 ± 0.01	15.59 ± 0.01	19.69 ± 0.02	19.62 ± 0.06	21.30 ± 0.10
V	17.42 ± 0.01	14.70 ± 0.02	19.43 ± 0.03	18.80 ± 0.02	19.51 ± 0.01
R	17.06 ± 0.01	14.18 ± 0.01	19.28 ± 0.03	18.33 ± 0.02	18.34 ± 0.02
I	16.71 ± 0.01	13.69 ± 0.01	–	–	–

Table 3. Optical and IR photometry of SN 1995G.

Date	JD	*U*	*B*	*V*	Δ(*V*)	*R*	*I*	*J*	*H*	*K*′	Instrument
28/02/95	49776.6	–	16.40	16.00	–	15.73	15.63	–	–	–	0
06/03/95	49782.6	15.96	16.33	16.02	0.03	15.76	15.56	–	–	–	1
30/03/95	49807.5	–	16.58	16.26	–	–	–	–	–	–	2
26/09/95	49986.6	–	18.81	18.07	–	17.41	16.95	–	–	–	0
14/10/95	50004.8	–	18.86	18.17	–	17.50	17.21	–	–	–	2
24/10/95	50014.6	–	18.91	18.23	–	17.59	–	–	–	–	0
24/10/95	50015.5	–	18.88	18.19	–	17.56	–	–	–	–	0
14/11/95	50035.5	–	–	18.43	0.05	17.83	17.41	–	–	–	3
22/11/95	50044.4	–	19.10	18.34	–	17.85	–	–	–	–	0
24/11/95	50045.5	–	19.03	18.47	–	17.87	–	–	–	–	0
17/01/96	50100.3	–	–	18.66	–	18.07	–	–	–	–	0
19/01/96	50101.6	–	19.25	18.66	–	18.11	17.77	–	–	–	4
18/02/96	50131.6	–	19.24	18.74	–	–	–	–	–	–	4
22/02/96	50135.6	–	–	–	–	18.03	17.82	–	–	–	1
04/09/96	50330.9	–	19.83	19.38	0.10	18.67	–	–	–	–	4
06/09/96	50332.8	–	–	–	–	18.64	18.53	–	–	–	4
19/11/96	50406.7	20.00	19.89	19.54	–	18.83	18.62	–	–	–	1
30/11/96	50418.3	–	–	–	–	–	–	18.3	17.7	17.2	a
02/01/97	50450.7	–	19.93	19.65	–	18.98	18.80	–	–	–	1
24/01/97	50473.1	–	–	–	–	–	–	18.5	18.2	17.6	a
28/03/97	50534.1	–	–	–	–	–	–	18.4	18.4	17.4	a
17/09/97	50709.4	–	–	–	–	–	–	19.1:	–	–	a
22/09/97	50713.9	–	21.27	21.44	0.40	20.22	20.14	–	–	–	4
17/11/97	50770.7	–	–	–	–	–	–	19.2	–	–	a
22/12/98	51169.8	–	–	≥21.4	–	≥21.2	–	–	–	–	1
03/01/99	51182.7	–	–	–	–	–	–	20.7	–	–	b
04/11/99	51486.8	–	–	–	–	≥22.1	–	–	–	–	5

0 = Asiago 1.82 m; 1 = Dutch 0.91 m; 2 = ESO 3.6 m + EFOSC1; 3 = NTT 3.5 m+EMMI; 4 = ESO 2.2 m + EFOSC2; 5 = Danish 1.54 m + DFOSC; a = ESO 2.2 m + IRAC2; b = NTT + SOFI.

brightness. The blue colour of the first spectrum is consistent with this belief (cf. Section 4).

At all wavelengths the light curves are relatively flat, decreasing by only 5 magnitudes in 2.5 years. The slopes of the light curves computed in different time intervals are given in Table 5. During the first months the slopes are steeper and then level out with time, until 1–2 years after the discovery they are as flat as 0.2–0.3 mag/100 d in all optical bands. A steepening in the luminosity decline was observed only after 650 days (about 0.5 mag/100 d). Apart from that, as we will see later, the light curve is very similar to that of SN 1988Z (Turatto et al. 1993).

Also, the colour evolution of SN 1995G (Fig. 4) is similar to that of SN 1988Z. Because of the cooling of the expanding layers, most 'normal' (non-interacting) SNe II show a rapid reddening after the explosion, and only the emergence of nebular lines makes the colour turn blue again (Patat et al. 1994). In SN 1995G instead we observe a slow increase in $(B - V)$ from 0.3 to 0.7 in ∼250 days, and then the colour curve flattens somewhat. Allowing for the large uncertainties, the SN seems to become blue again about 2.5 years after the discovery. It is interesting to note that the colour curves of other SNe IIn, SN 1988Z (Turatto et al. 1993; Aretxaga et al. 1999) and SN 1997cy (Turatto et al. 2000), show similar properties, while the few points of SN 1996L (Benetti et al. 1999) indicate a more rapid evolution.

3.2 The absolute and bolometric light curves

Adopting the distance modulus $\mu = 34.32$ and a total absorption $A_B = 0.20$ (cf. Section 4.2), we can calculate the absolute magnitudes near maximum. The values are $M_B \sim -18.19$,

$M_V \sim -18.47$, $M_R \sim -18.72$ and $M_I \sim -18.85$. Fig. 5 shows the comparison of the absolute V light curve of SN 1995G with those of other representative SNe II. The close coincidence with SN 1988Z is remarkable.

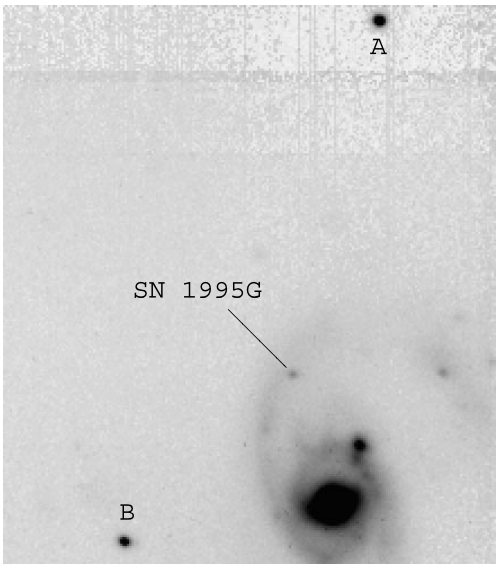

Figure 2. SN 1995G and the IR local sequence (J- band image, taken with ESO 2.2 m + IRAC2 on 1996 November 30). Note that star A coincides with star 1 of the optical sequence. IR magnitudes of the stars are given in Table 4.

Table 4. IR magnitudes for stars of the local sequence.

Filter	A	B
J	15.88 ± 0.07	16.32 ± 0.02
H	15.40	15.60 ± 0.02
K'	–	15.52 ± 0.05

Table 5. Decline rates (mag/100 d) of SN 1995G.

Δ (Days)	γ_B	γ_V	γ_R	γ_I
0–215	1.19	1.07	0.80	0.65
215–680	0.25	0.33	0.31	0.36
680–940	0.51	0.68	0.47	0.51

In order to compute the energy budget of SN 1995G and to simplify the comparison with theory, it is useful to determine the bolometric light curve. Unfortunately, no detections at UV, X-ray or radio wavelengths are available, and we stress that in the case of SN 1988Z the contributions at these wavelengths were important (Aretxaga et al. 1999). Actually, the position of SN 1995G was targeted with the VLA on 1995 June 22 (Van Dyk, private communication), but no radio emission was detected.

The available data range from U to K' bands, with much denser sampling at optical wavelengths. U-band data are available only at two distant epochs. We have estimated the contribution at intermediate epochs interpolating the U-band contribution to the total emission between the two available epochs. Unfortunately, near-IR observations start only when those in the U-band cease, that is after 600 days.

The *UBVRI* bolometric light curve is shown in Fig. 6, along with those of other SNe IIn and that of SN 1987A. As a reference, we note that the luminosity of SN 1995G at the time of the first observation is only 5 times that of SN 1987A at the secondary maximum, while after 2 years it is 200 times brighter. Note that the latter are lower limits to the ratio of the bolometric luminosities, because in the case of SN 1987A the IR contribution is included. The *UBVRI* curves of SN 1995G and SN 1988Z (Aretxaga et al. 1999) are very similar. SN 1997cy, to date the most luminous type II SN, had a much faster decline rate, and indeed after day 600 SN 1995G it outshines SN 1997cy.

Since IR observations of SN 1995G are available only at late epochs, their contribution to the energy budget immediately after the SN explosion is unknown. We note, however, that around day 640 after the discovery, when we have the broadest photometric coverage from U to K', the cumulative contribution of J, H, K' bands is about 50 per cent that of *UBVRI*. Our data indicate that the contribution of the near-IR increases with time, because the decline rates of infrared light curves appears to be slower than the optical ones.

We note that our IR observations of SN 1995G in the interval between days 640 and 750 do not show the rise of the K' continuum detected by Fassia et al. (2000) for the type IIn SN 1998S and attributed to emission from pre-existing, warm dust in the circumstellar material.

4 SPECTROSCOPY

4.1 The spectral evolution

The spectral evolution of SN 1995G during the first 2.5 years after the explosion is shown in Fig. 7. The first spectrum was taken

Table 6. Spectroscopic observations of SN 1995G.

Date	JD	Days after discovery	Instrument	Grism or grating	Resol. (Å)	Exp. (min)	Range (Å)
25/02/95	49773.5	2	Lick	600,1200,600	7,4,7	7.5,7.5,7.5	3380–7300
30/03/95	49807.5	36	ESO3.6+EF.1	B300,O150,R300	18.4,7.6,21.5	10,15,10	3715–9805
14/10/95	50004.9	233	ESO3.6+EF.1	B300	18.4	15	3745–6940
31/10/95	50021.6	250	As1.82+B&C	150	23	60	4530–8305
14/11/95	50035.7	264	NTT+EMMI	gm#3	7.8	30	3860–8390
19/01/96	50101.7	330	ESO2.2+EF.2	gm#1,gm#6	36,11.2	30,30	3325–9215
18/02/96	50131.6	360	ESO2.2+EF.2	gm#6	11.2	60	4450–7060
06/09/96	50332.5	561	ESO2.2+EF.2	gm#3,gm#5	8.8,10.8	30,30	3220–9250
19/12/96	50436.5	665	ESO1.5+B&C	gt#25	8	60	3515–9280
17/02/97	50496.6	725	ESO1.5+B&C	gt#15	10	60	3085–10640
22/09/97	50713.9	942	ESO2.2+EF.2	gm#5	11	60	5205–9305

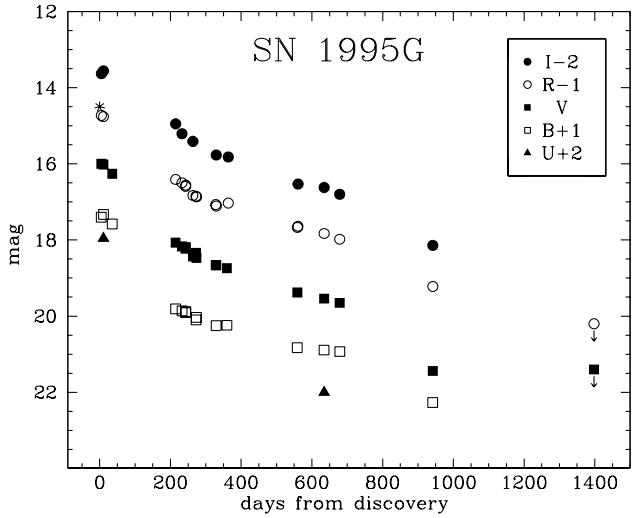

Figure 3. Light curves of SN 1995G in *B*, *V*, *R* and *I* bands. The two *U* points are also reported. The asterisk refers to the discovery unfiltered magnitude (IAU Circ. 6138) plotted on the same scale as *R* photometry.

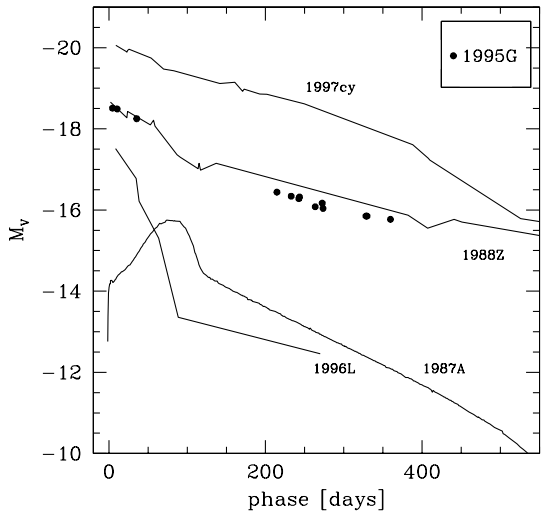

Figure 5. Absolute *V* light curve of SN 1995G compared with that of SN 1988Z (IIn, Turatto et al. 1993), SN 1997cy (IIn, Turatto et al. 2000), SN 1987A (II, Patat et al. 1994, and references therein) and SN 1996L (IId, Benetti et al. 1999).

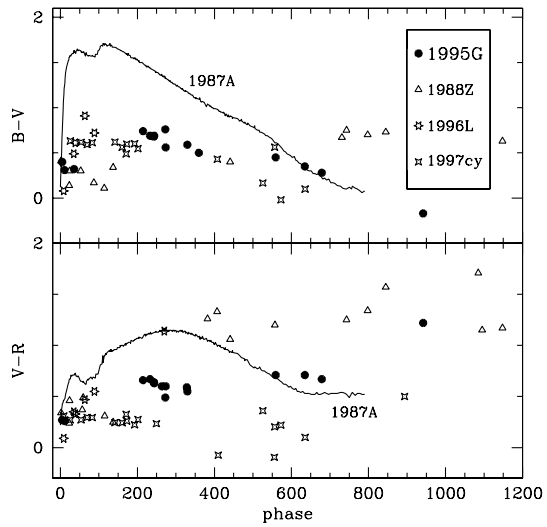

Figure 4. Top: $(B - V)$ colour evolution for SN 1995G compared with SN 1988Z, SN 1996L, SN 1997cy and SN 1987A; bottom: $(V - R)$ colour evolution for the same objects.

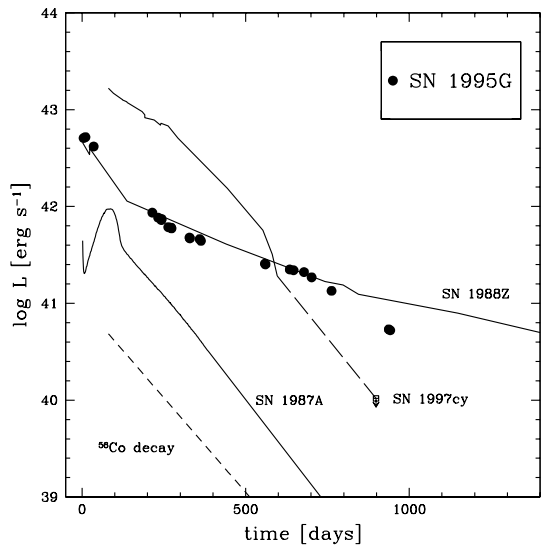

Figure 6. The *UBVRI* bolometric light curve of SN 1995G (dots) compared to that of SN 1987A (*UBVRIJHKL*, Catchpole et al. 1987, 1988, 1989), SN 1997cy (*UBVRI*, Turatto et al. 2000) and SN 1988Z (*BVR*, Aretxaga et al. 1999). The decline rate of ^{56}Co is reported for reference. The dashed tail of SN 1997cy connects the last detection to an upper limit, and therefore the true decline may be steeper than that drawn here.

within two days from the discovery (Filippenko & Schlegel 1995). It shows a relatively blue continuum ($T_{\rm eff} = 8800$ K after dereddening, cf. Section 4.2) with relatively narrow Balmer P Cygni features superimposed on broader emission components. The overall intensity ratio of Hα/Hβ is 1.58, lower than Case B recombination (2.8), while the intensity ratios of the individual components (cf. Section 4.4) are very difficult to measure. The departure from simple recombination is probably the result of line formation in an extended atmosphere where the Balmer lines may have significant optical depths. The P Cygni absorption minima are displaced by about 700 km s^{-1} from the emission-line cores both for H and Fe II lines.

The next spectrum, taken about 1 month later, is similar, with a continuum temperature $T_{\rm eff} = 7000$ K and several narrow P-Cyg lines of H, O I, Ca II and Fe II (see Section 4.3). Neither He nor Na I D lines are visible. The most evident difference with respect to the first spectrum is in the Hα/Hβ ratio, which has now increased to 3.0. Again this can be understood to result from the decrease of the optical depths of the Balmer lines as the density decreases. Indeed, in the same period the ratio of the equivalent widths does not change significantly [EW(Hα)/EW(Hβ) = 3.0 and 3.2, respectively]. Though conspicuous, the emission lines in the early spectra account for only about 4 per cent of the total optical flux, and have only a small influence on the SED.

The SN was then recovered 8 months after discovery when the spectrum had noticeably changed. The continuum was redder and fainter, and dominated by emission lines of Hα, Hβ and the infrared Ca II triplet. He I lines (e.g., 7065 Å) appear and remain clearly visible for about 1 year, but contrary to other lines they do

not show a blueshifted absorption. The He I 5876-Å line is blended with Na I D, the latter having the narrow P Cygni component. The very late spectrum shows only Balmer lines in emission (and probably IR Ca II). It should be noted that the galaxy contribution to the spectrum is not completely removed when the SN fades and the spectra are contaminated by the unresolved [S II] 6717, 6731 Å doublet, coming from an underlying H II region. Probably the background contaminates also the Hα narrow component with a (small) contribution to the total flux of the line. It is remarkable that during all the evolution there is a monotonic increase of the Balmer decrement.

In Fig. 8 we compare the spectrum of SN 1995G taken on 1995 March 30 with those of other SNe IIn. Despite the general similarity, the spectrum shows important differences with both SN 1997cy and SN 1988Z. The linewidths of these two objects are much broader than those of SN 1995G, implying expansion velocities of about 15 000 km s^{-1} instead of 4000–5000 km s^{-1}, hence probably higher explosion energies (Aretxaga et al. 1999; Turatto et al. 2000). The

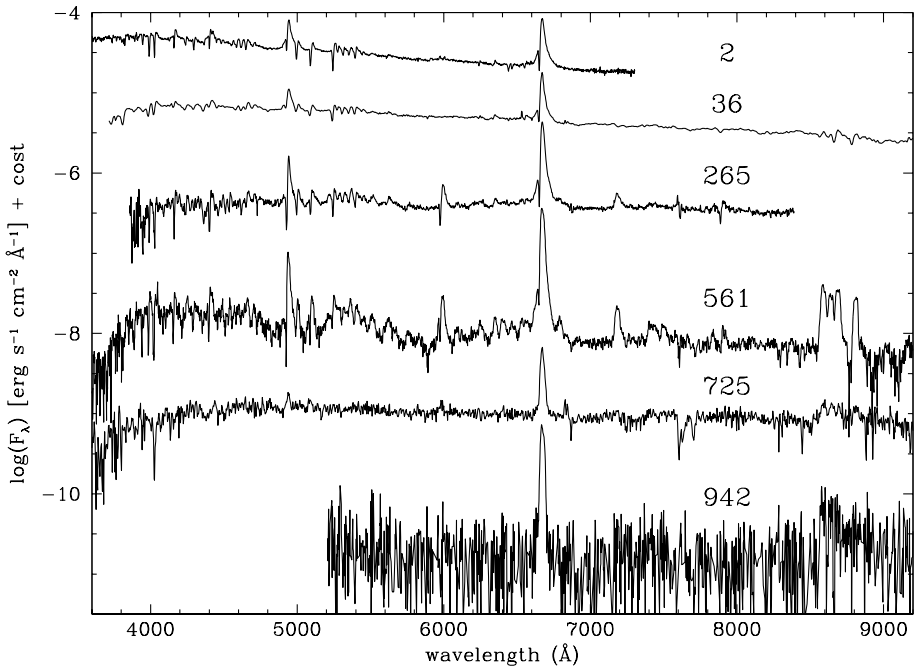

Figure 7. Spectral evolution of SN 1995G. The spectra are in the observer rest frame, and the days from discovery are reported near each spectrum. On day 725 the atmospheric absorptions could not be removed. In combining spectra, priority has been given to those of higher resolution.

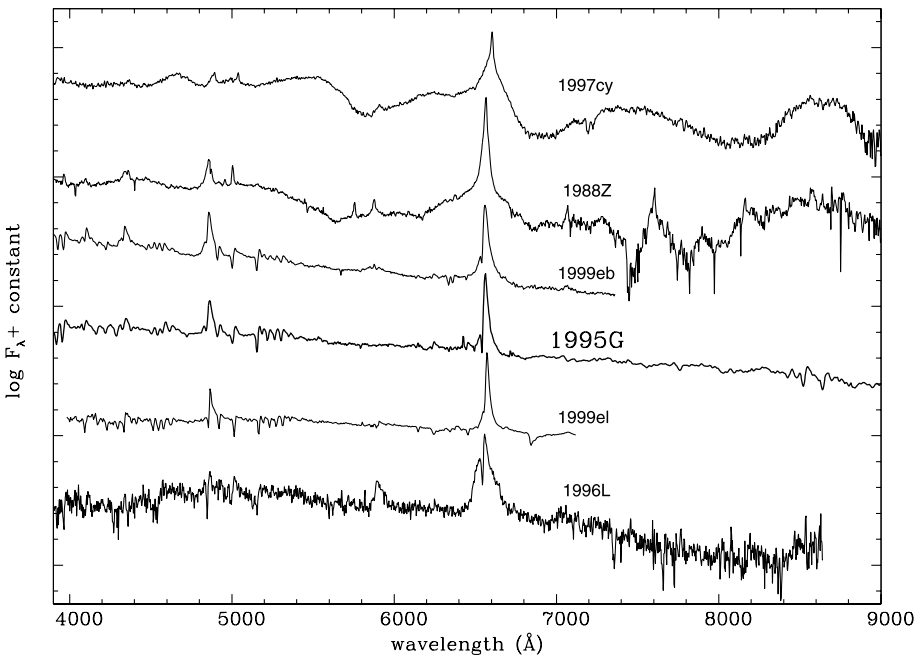

Figure 8. Comparison between the spectrum of SN 1995G taken on 1995 March 30 (36 days after the discovery) and the spectra of SN 1997cy (39 days), SN 1988Z (4 months), SN 1999eb (2 months), SN 1999el (18 days) and SN 1996L (2 months). All spectra are in the parent galaxy rest frames.

fact that SN 1995G and SN 1988Z have different kinematics of the ejecta, but nearly identical broad-band light curves and overall luminosity evolution (Fig. 6) must be connected to the different densities of the respective circumstellar media (cf. Section 5).

The spectrum of SN 1995G more closely resembles that of SN 1999eb taken 2 months after the discovery, and SN 1999el taken 18 days after the discovery (see Fig. 8). They have similar continua and strong emission lines with similar profiles. Curiously, the light curves of these objects having strong spectral similarities to SN 1995G are steeper than that of SN 1995G, as shown by sparse unpublished observations from our archive.

In recent years several SNe have shown narrow P Cygni absorptions. As we mentioned before, a number of SNe, sometimes dubbed IId or IIsw, show these features over an otherwise normal, broad-line photospheric spectrum. The spectrum of one of these, SN 1996L (Benetti et al. 1999), is shown in Fig. 8. It has been argued that in all these cases the narrow P Cygni features originate in a slowly expanding shell of gas which has been ejected shortly before the explosions. In spite of the fact that these SNe show spectroscopic signature of ejecta–CSM interaction, they have light curves that decline as steeply as typical linear SNe II, and hence differ from SN 1995G.

4.2 The recession velocity and the interstellar absorption

The recession velocity of the host galaxy at the location of the SN, $v_h = 4911 \pm 70\,\mathrm{km\,s^{-1}}$, has been derived from the narrow emission lines (Hα, Hβ, [N II] and [O III]) arising from the H II regions surrounding the SN and measured on the spectrum of better resolution. This value is consistent with the nuclear velocity of NGC 1643, $v_{\mathrm{helio}} = 4850 \pm 29\,\mathrm{km\,s^{-1}}$ (Huchra et al. 1993), since SN 1995G is located in an outer arm of the parent galaxy.

Interstellar absorption lines of Na I D are not clearly detected neither at the rest wavelength nor in the parent galaxy rest frame, suggesting that the reddening cannot be particularly strong. The values of Galactic absorption given by Schlegel, Finkbeiner & Davis (1998) and in RC3 are in good agreement, respectively $A_B^g = 0.22$ and 0.19. In the following we will adopt for SN 1995G a total extinction $A_B = 0.20$, assuming therefore no absorption within the parent galaxy.

4.3 Line identifications

The line identifications have been made on two good signal-to-noise spectra taken on day 36 (1995 March 30) and day 561 (1996 September 6). The identifications are shown in Fig. 9.

At early times the strongest features are the H I Balmer lines characterized by broad emissions on top of which are narrow P Cygni features. Fe II multiplet lines are also identified as absorption features in the bluest part of the spectrum (cf. Fig. 9). Ca II H and K, and its IR triplet are also present and resolved in the multiplet components, as well as the O I lines at 7772 and 8446 Å. Two emissions at about 6250 and 5530 Å (not marked in the figure) might be attributed to Sc II. Noticeable is the absence at this epoch of Na I D and He I lines, which will appear only later (cf. Section 4.5). Unlike the case of SN 1988Z, very high-ionization (coronal) lines are not detected.

Numerous lines are identified also at the late epoch. Because of the small velocity of the emitting layers, the individual components of the IR Ca II triplet are resolved, as well as the strong O I 8446-Å emission. The strength of this line and the uncertain presence of other oxygen lines (such as O I 7772 Å) is suggestive of the Lyβ pumping mechanism (Grandi 1980). [O I] 6300, 6363 Å is not unambiguously identified because of the presence of other lines. Fe II is still present in numerous multiplets, while the presence of [Fe II] lines is not certain. In contrast with early spectra, many He I emissions lines become visible; among these the most obvious are at 7065, 6678, 5876, 5015, 4471 Å, none of which shows the

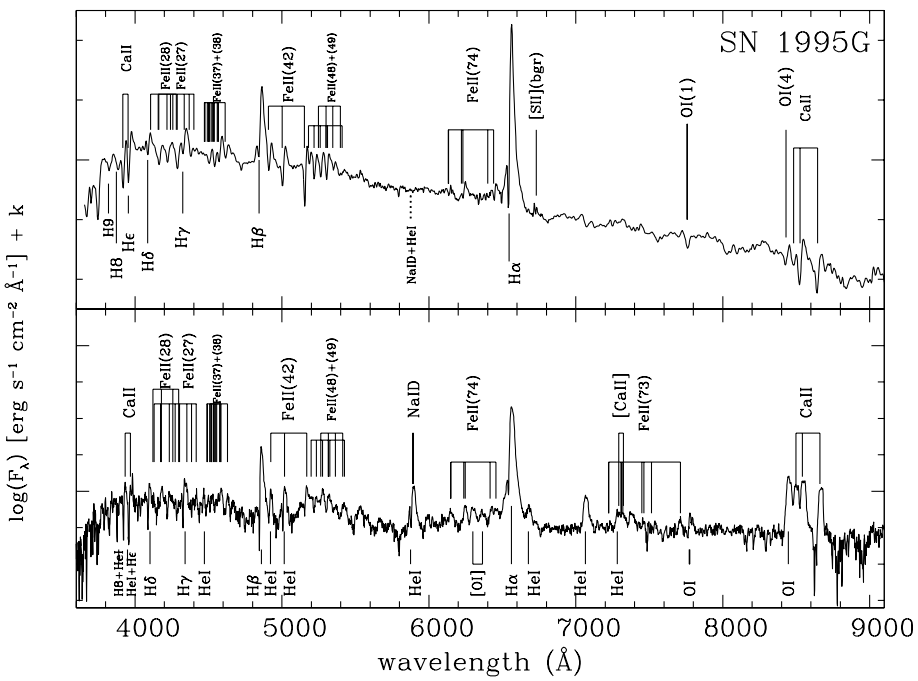

Figure 9. Line identifications in the spectra of SN 1995G. Top: early spectrum taken on 1995 March 30. The vertical lines mark the minima of P Cygni absorptions, blueshifted by $750\,\mathrm{km\,s^{-1}}$ with respect to the line rest wavelengths. Bottom: late spectrum on 1996 September 6. Marked are the cores of the emissions. The spectra are blueshifted to the host galaxy rest frame.

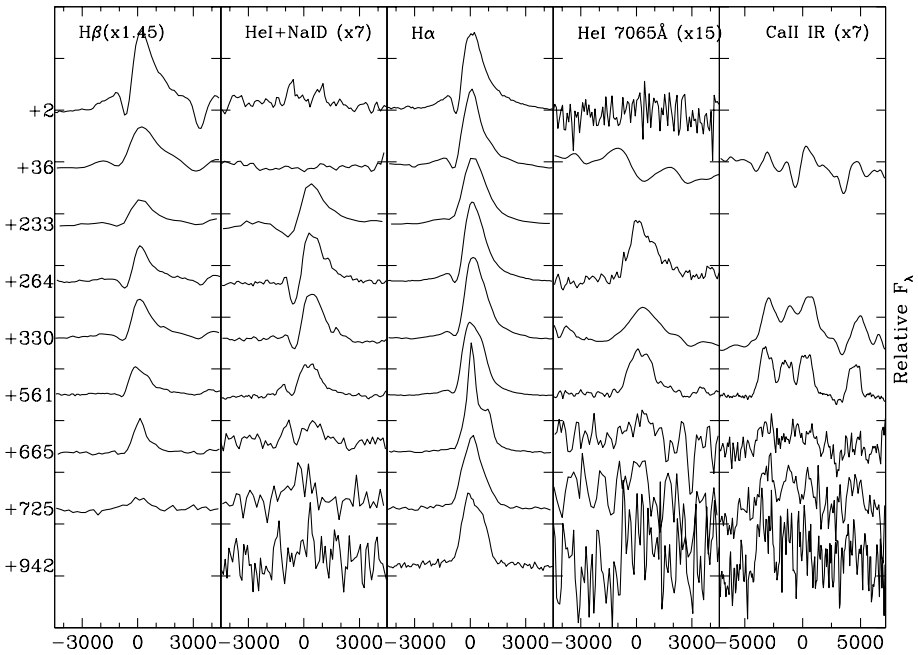

Figure 10. Evolution of the profiles of the main spectral lines of SN 1995G. The peak on the red wing of Hα in the spectrum taken 665 days after SN discovery is [N II] due to the background. The Hα lines are normalized at their peak; the other lines are normalized with Hα and then multiplied by a constant.

P Cygni absorption component still visible in other lines. The 5876-Å line is blended with Na I D.

4.4 The profile and evolution of the Balmer lines

The line profiles of Hα and Hβ are complex and evolving with time. At early phases the lines show strong and narrow emission cores with blue absorptions superposed on broad wings. The relative intensities of the components change, and the absorption features completely disappear at about 2 years. The temporal evolution is summarized in Fig. 10, together with that of other significant lines.

The expansion velocities at the photosphere derived from the P Cygni minima are reported in Table 7. The velocities measured for Hα are of the order of 700–800 km s^{-1}, thus indicating either that the kinetic energy of the ejecta is very small, as in the case of SN 1997D (Turatto et al. 1998; Benetti et al. 2001), or that they arise from an outer, slowly expanding shell, as in the case of SNe 1994aj (Benetti et al. 1998) and 1996L (Benetti et al. 1999). The expansion velocities measured from the Fe II 5169-Å absorption are on average slightly lower, about 600 km s^{-1}. The typical full-width half-depth of the Hα absorption lines is around 400–450 km s^{-1} (cf. Table 8). Contrary to the absorption lines of normal SNe which form just above the receding photosphere (and hence show a progressive redshift of the minima), the absorptions of SN 1995G remain at constant location in wavelength.

To disentangle the different components of Hα, we performed a multicomponent Gaussian fit of the lines. Within the first two years at least two emission components and a narrow blueshifted P Cygni absorption are required to get a reasonable fit. However, the fitting of spectra of higher signal-to-noise ratio and resolution requires a third emission component. The fitting was performed using the deblending option of the *splot* command in IRAF. Apart from giving an inital guess for the position, FWHM and peak intensity of each component, no additional constraints were imposed. The FWHM and fluxes of the components of Hα are shown in Table 8. Although

Table 7. Expansion velocities from the minima of P Cygni absorptions.

Date	Days after discovery	v(Hα) (km s^{-1})	v(Fe II 5169 Å) (km s^{-1})
25/02/95	2	710	510
30/03/95	36	840	750
14/10/95	233	750:	600:
31/10/95	250	–	630:
14/11/95	264	670	470
19/01/96	330	620	470
18/02/96	360	670	590
06/09/96	561	750	800

we are aware that fitting multiple Gaussian components to the composite spectral profile is somewhat arbitrary, we believe that it is safe to conclude that the observed emission lines arise from regions with significantly different characteristic velocities.

From Table 8 we note a slow monotonic evolution of the FWHM(Hα). The broad component has a FWHM of 4000–4500 km s^{-1} in the first spectra, decreasing to about 3000 km s^{-1} after 1 year and to 2200 km s^{-1} after 2 years. The intermediate component also declines from about 2000 to 1200 km s^{-1}. The narrow component is resolved in the early spectra, while at later epochs the linewidth is below the spectral resolution. The evolution in width and intensity of this narrow component demonstrates that it is not due the galaxy background, although some contamination is possible (cf. the [N II] 6584-Å emission on day 665, Fig. 10). At the last epoch (942 days) the Gaussian fit fails because the profile is clearly boxy with FWZI = 2500 km s^{-1}.

The total Hα flux, as well as the fluxes of the individual components, shows an overall decline with time. Small-scale fluctuations in the Hα flux are to be ascribed to uncertainties in the absolute flux calibration and/or to uncertainties in the fitting. The comparison of the Hα integrated luminosity evolution of

Table 8. Three-component Gaussian deblending of Hα, and Balmer decrements.

Date	Phase	FWHM* (Hα) [km s^{-1}]				flux† (Hα) [10^{-16} erg cm^{-2} s^{-1}]					Balmer decrement	
	[days]	broad	interm.	narrow	abs.	broad	interm.	narrow	abs.	total	obs.	†
25/02/95	2	4150	1850	950	400	416	530	219	−138	1170	1.58	1.50
30/03/95	36	4600	2100	700	400	226	373	225	−75	824	3.03	2.89
14/10/95	233									360	5.45	5.20
31/10/95	250									524	5.35	5.09
14/11/95	264	3100	1300	250	450	202	320	11	−68	533	5.61	5.35
19/01/96	330	3000	1200	100:	450	197	277	25	−59	729	5.52	5.26
18/02/96	360	3450	1400	unres.	450	138	321	11	−68	470	6.02	5.74
06/09/96	561									531	6.32	6.02
19/12/96	665	2200	1150	unres.	450:	85	124	53	−14:	262	6.56	6.24
17/02/97	725									176	12.57	11.97
22/09/97	942	Boxy(FWZI ∼ 2500)								116		

* deconvolved for the spectral resolution.
† corrected for reddening.

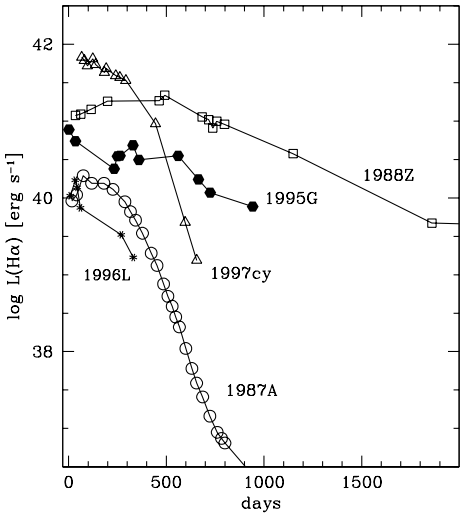

Figure 11. The evolution of the Hα luminosity for SN 1995G and other CSM interacting SNe, SN 1988Z, SN 1997cy and SN 1996L. Also, SN 1987A is reported for comparison. A typical error in $\log L(\mathrm{H}\alpha)$ is 0.3.

SN 1995G with that of other SNe (Fig. 11) shows that SN 1995G is similar to the CSM-interacting type IIn rather than to the radioactivity-powered normal SNe II, e.g., SN 1987A. We note, however, that while the *UBVRI* bolometric light curve of SN 1995G was nearly identical to that of SN 1988Z (Fig. 6), the Hα flux is about 0.8 dex fainter.

4.5 He I lines

He I emission lines are not visible in the first spectra (cf. Figs 7 and 10). They emerge only after day 200, reach the maximum intensity between 8 and 20 months, and then disappear. In the day 561 spectrum, when He emissions reach the maximum relative intensity, we identify He I 4471, 6678 and 7065 Å. None of these lines show evidence of an absorption component. Other He I lines are probably blended with lines of other ions, e.g., with Fe II 4921 and 5015 Å. In particular, He I 5876 Å is blended with the Na I D P Cygni feature.

For the clean 7065-Å emission we measure a FWHM velocity between 1200 and 1800 km s^{-1}, close to that of the intermediate component of the Balmer lines. The flux of this line is about 3×10^{-15} erg cm^{-2} s^{-1}, between days 250 and 561. In the spectrum of day 665 the flux is one order of magnitude smaller (about 3×10^{-16} erg cm^{-2} s^{-1}); afterwards the line was not detected. Other He I lines seem to have a similar evolution.

The strength of the He I 7065-Å line with respect to other lines, e.g., 5876 Å, suggests that non-thermal processes are at work. A similar evolution of He lines was observed in SN 1996L (Benetti et al. 1999).

5 DISCUSSION

The light curves of the type II SN 1995G presented in Section 3 show relatively high luminosity and very slow luminosity declines. The absolute magnitude ($M_V \sim -18.47$) is similar to that of SN 1988Z and SN 1994W (Sollerman, Cumming & Lundqvist 1998), two objects sharing some of the properties of SN 1995G.

The slow fading of SN 1995G persists well beyond 5–6 months, an epoch at which the light curves of normal SNe II, powered by the radioactive decay of ^{56}Co, decline at about 1 mag/100 d (Figs 5 and 6). Therefore, another source of energy in addition to the radioactive decay is needed to power the light curve of SN 1995G. The similarity at all epochs SN 1988Z suggests that also in this case the surplus energy comes from the transformation of kinetic energy of the ejecta into radiation owing to interaction with a dense CSM.

Aretxaga et al. (1999) have proposed that in the case of SN 1988Z most of the energy have been emitted as X-rays and as ionizing radiation. They estimated that the total radiated energy was as high as 10^{52} erg, suggesting complete reprocessing of the mechanical energy of the ejecta in only a few years. Unfortunately, no X-ray observation is available for SN 1995G. The ionization energy computed from the Hα luminosity (Aretxaga et al. 1999) is considerably smaller for SN 1995G than for SN 1988Z, because of the weaker line emission (Fig. 11). However, despite significant differences in the Hα luminosity, the bolometric luminosities of the two SNe are very similar. The radiated energy of SN 1995G integrated over the 3 years of observations is almost the same as in SN 1988Z in the same period (10^{50} erg in *BVR*).

The optical light curves of SN 1988Z, the X-rays and Hα emission, and the linewidth evolution are reproduced by a model in which the ejecta is interacting with a dense ($n = 10^7$ cm^{-3}) and homogeneous CSM (Terlevich et al. 1992; Aretxaga et al. 1999). In these conditions the SN remnant evolves very rapidly, and radiative cooling becomes important well before the thermalization of the ejecta. The ejecta–CSM interaction causes the formation of a hot

shocked shell between two shock waves: a forward shock ($v \approx 10\,000\,\mathrm{km\,s^{-1}}$) encountering and heating the CSM to a temperature of about 10^9 K, and a slow reverse shock ($v \approx 1000\,\mathrm{km\,s^{-1}}$) which thermalizes the SN ejecta to a temperature of about 10^7 K. A high flux of X-ray photons is produced in the high-density material shock front, while the cooling shocked gas reinforces the intensity of Hα components. The reference model by Terlevich et al. (in preparation) of the interaction of the ejecta with a circumstellar shell ($n_\odot = 10^7\,\mathrm{cm^{-3}}$ and $Z = 10\,Z_\odot$) does not fit completely the observations of SN 1995G. In particular, the observed Hα luminosity of SN 1995G after 230 days (1 t_{sg}) is fainter by a factor of 10, and the Balmer decrement is too steep. Indeed, these differences are not surprising, because type IIn SNe exhibit considerable heterogeneity, indicating that the physical conditions and/or the geometry of the interaction can be very different. For example, SN 1988Z remained visible for over 10 years, while SN 1994W dropped in luminosity after 4 months, probably because the interaction ceased earlier. SN 1997cy, the brightest SN IIn rapidly faded below the detection limit after 2 years (Turatto et al. 2000).

The first spectrum of SN 1995G shows a continuum corresponding to $T_{BB} = 8800$ K, a temperature close to that of SN 1987A a couple of days after the explosion, supporting the idea that SN 1995G was discovered soon after the explosion (Section 3.1). On the other hand, the small temperature variation over the first month [$T_{BB}(36\,\mathrm{d}) = 7000$ K] gives the opposite indication. The spectra show some distinctive feature compared to those of SN 1988Z, which shared similar bolometric evolution. The narrow absorption components were never detected in the spectra of SN 1988Z, although this might be due to the modest spectral resolution of those observations.

The spectra of SN 1995G are very similar both as line ratios and profiles to those of SN 1994W around maximum (Sollerman et al. 1998). In particular, Hα shows the same velocity profiles with absorption minima blueshifted by similar amounts (cf. Fig. 10 with fig. 3 in Sollerman et al. 1998). Other ions, e.g., Ca II and Fe II, show similar line profiles. Instead, the blackbody temperature of SN 1995G is lower, and two days after the discovery it corresponds to that of SN 1994W on day 80.

From the blackbody fits and the bolometric luminosity we can derive the photospheric radii on days 2 and 36, which are of 1.1×10^{15} and 1.6×10^{15} cm, respectively.

Up to about 1 year the P Cygni profiles of Hα and Fe lines are rounded, and the narrow emission and absorption components are symmetric. This indicates that optical depths of these lines are $\gg 1$, and that the lines are scattering-dominated and originate in a rather thin shell close to a (pseudo)photosphere. Rybicki & Hummer (1978) showed that in this situation of an expanding shell the optical depth in a line depends on the velocity gradient. Fransson (1984), elaborating on this, presented a precise expression for the optical depth, which was then used in the specific case of SN 1994W by Sollerman et al. (1998) to derive a lower limit to the density in the shell under the assumption that the lines had a large optical depth because their profiles were rounded or parabolic (Mihalas 1978). The case is, in this respect, very similar to that of SN 1995G; thus we can use the expression $n_H \gg 3 \times 10^8 v_3 r_{15}^{-1}\,\mathrm{cm^{-3}}$, where v_3 is the shell velocity in units of $10^3\,\mathrm{km\,s^{-1}}$, and r_{15} is the shell radius in units of 10^{15} cm. Assuming that the shell radius is close to that of the photosphere, using the values of v_3 derived from the minima of the absorptions, we get $n_H \gg 10^8\,\mathrm{cm^{-3}}$, consistent with the absence of forbidden lines. The density of the slowly expanding material in SN 1995G is therefore similar to that of SN 1994W but higher than in SN 1988Z, for which the ratio of [O III] 4363, 4959 and 5007 Å lines indicate densities $n_e \geq 10^7\,\mathrm{cm^{-3}}$ (Filippenko 1991; Statakis & Sadler 1991).

Another distinctive characteristic of some SNe IIn, e.g., SN 1988Z, SN 1995N (Benetti, Bouchet & Schwarz 1995; Turatto et al. in preparation) and SN 1986J (Turatto et al. 1993), is the presence of narrow emission lines of very high ionization (e.g., [Fe VII], [Fe X]) which are direct evidence of energy dissipation in powerful shock waves. In SN 1995G such lines are not present.

We noted in Section 4 that it is possible to identify gas with different kinematics. The results of a multicomponent fit for SN 1995G have been summarized in Table 8. Compared to the expansion velocity of the broadest component of SN 1988Z (FWHM = $15\,000\,\mathrm{km\,s^{-1}}$), the broad component in SN 1995G is much slower (FWHM $< 5000\,\mathrm{km\,s^{-1}}$), while the other components are similar. This implies that the fast-moving ejecta photoionized by the hard radiation of the shock move more slowly, justifying the absence of very high-ionization species.

Similarly to SN 1996L (Benetti et al. 1999), after day 200 high-excitation He lines emerge. The low temperature of the envelope suggests that these lines result from non-thermal processes. The unusual relative strengths of the He I lines probably owe their origin to excitation by a radiative shock in the dense or clumpy wind, with the consequent large optical depth in the He I 3889-Å line. Such line ratios have been observed in some symbiotic stars by Proga, Mikolajewska & Kenyon (1994), who appealed to the calculations of Almog & Netzer (1989) to show that large optical depths of He I 3889 Å combined with high densities of 10^8–10^{10} cm may produce these unusual line ratios. We have demonstrated the plausible existence of high densities at intermediate velocity probably associated with shock propagation. The bump in the Hα light curve during the same interval may result from the same shock excitation.

After 2 years, the absorption components disappear and Hα evolves to a boxy profile. Simultaneously, the Hα luminosity declines and the light curves become steeper, but still not as much as the decay rate of ^{56}Co. This may suggest that the interaction is fading. Something similar happened in SNe 1994aj (Benetti et al. 1998) and 1996L (Benetti et al. 1999), in which the narrow P Cygni profiles of gradually disappeared, leaving broad boxy emissions. In the case of SN 1996L, we observed the progressive development of the narrow features first as pure emissions, and later as P Cygni structures, when significant recombination took place. After 100 days the lines broadened, and the absorption progressively disappeared. This has been interpreted as the onset of the interaction of the ejecta with an outer shell which is progressively swept away. The analysis of the timing of these phases led to the conclusion that the shell was produced by a wind episode that started 9 years before the explosion and lasted 6 years. Benetti et al. (1999) noticed that SNe 1994aj and 1996L had linear light curves in the early 100 days, which is indirect evidence of low-mass, wind-deprived envelopes.

The case of SN 1995G is different. The light curve remains very flat since the discovery, indicating that the interaction with the CSM started soon after the burst, and is still continuing at the time of our last observation on day 942. Therefore, if the CSM is due to a stellar wind from the progenitor, a strong wind persisted almost to the time of the explosion. From the duration of the interaction, given a wind velocity of $750\,\mathrm{km\,s^{-1}}$ and a maximum expansion velocity of the ejecta of $4500\,\mathrm{km\,s^{-1}}$ (Fig. 10), we deduce that the wind episode started at least a dozen years before the burst. The dense CSM could be due also to the presence of a companion

which might have stripped gas from the precursor or might have lost its own envelope.

The fact that the P Cygni profile is already well developed at the discovery, contrary to the case of SN 1996L, indicates that the recombination of the shell took place earlier, probably because of higher densities ($n_{\rm H} \gg 10^8\,{\rm cm}^{-3}$). After 2 years, however, most of the slowly expanding shell has been swept away by the forward shock, the optical depth of the unshocked material is low, and the line profiles show only the boxy shape due to the shock. The simultaneous decrease of brightness (increase of decline rate of the light curves) can be evidence of a steepening of the density profile in CSM shell. Yet, up to 3 years after the discovery, there is evidence that the residual interaction between the SN ejecta and CSM has not completely ceased.

Thus, SN 1995G seems to be an intermediate case between SN 1988Z interacting with a dense CSM from the early stages after the explosion, and less extreme objects like SNe 1994aj and 1996L in which interaction with a shell of material ejected a few years before the explosion were limited in time.

5.1 Progenitor mass loss

In Section 5 we pointed out that the Terlevich et al. (in preparation) model of the interaction of the ejecta with a dense, uniform density gas, which reproduces the observations of SN 1988Z, does not fit all the observables of SN 1995G. Chugai & Danziger (1994) presented calculations of the dynamical interaction of the ejecta of SN 1988Z with a dense clumpy circumstellar wind ($\rho \propto r^{-2}$). Following the latter approach, we can derive some important parameters of the progenitor.

We assume that the velocity of the broad Hα emission is representative of the velocity of the ejecta, since this component is supposed to originate in the shocked ejecta.

The interaction between the ejecta and the progenitor's wind follows two distinct phases. Initially, the outer part of the SN ejecta, having a power-law density distribution, collides with the wind. This is the so-called free expansion phase. In this phase the shock velocity (which is observed as the velocity of the broad component of Hα) is given by

$$v = 7.46\times10^{8} E_{51}^{2/5} \left(\frac{M_{\rm ej}}{{\rm M}_\odot}\right)^{-1/5} {\rm w}_{16}^{-1/5} t_{\rm yr}^{-1/5} [{\rm cm\,s^{-1}}], \quad (1)$$

where E_{51} is the kinetic energy of the ejecta in units of 10^{51} erg, $t_{\rm yr}$ is the time elapsed since the explosion in years, $w = \dot{M}/u_{\rm w}$ is the wind density parameter, $u_{\rm w}$ is the wind velocity, and $w_{16} = w/10^{16}\,{\rm g\,cm^{-1}}$. A lower limit for w can be obtained from the general expression for the luminosity of the shock wave:

$$L = \frac{1}{2}\psi w v^3. \quad (2)$$

Here L is the SN luminosity (which is dominated by the interaction), and ψ is the efficiency of conversion of mechanical into optical energy.

In the case of SN 1995G at $t \approx 0.2$ yr, we estimate $L \approx 4\times10^{42}\,{\rm erg\,s^{-1}}$ (with a considerable uncertainty, because of the paucity of observed data at this epoch) and $v \approx 4000\,{\rm km\,s^{-1}}$. If we assume $\psi = 1$, equation (2) gives $w_{16} = 12.5\,{\rm g\,cm^{-1}}$. For a wind velocity $u_{\rm w} = 10\,{\rm km\,s^{-1}}$, typical of a red supergiant (RSG), we get $\dot{M} = 0.002\,{\rm M_\odot\,yr^{-1}}$, which is a lower limit because in general $\psi < 1$. Such large $\dot{M}$ results from the fact that L is large but v is small. In the case of SN 1988Z, which has the same L but $v = 17\,000\,{\rm km\,s^{-1}}$, $\dot{M} = 2.6\times10^{-5}\,{\rm M_\odot\,yr^{-1}}$. From equation (1) and $w_{16} = 12.5\,{\rm g\,cm^{-1}}$ we obtain the ejecta mass of SN 1995G: $M_{\rm ej}/{\rm M_\odot} \simeq 9\times E_{51}^2$. So, if $E \simeq 10^{51}$ erg, $M_{\rm ej} \simeq 9\,{\rm M_\odot}$.

Eventually, the outer, power-law part of the ejecta overtakes the wind, and the interaction is then between the wind and the inner part of the ejecta, which has a flat density profile. In this regime, called the blast wave phase (Chugai & Danziger 1994), the velocity is

$$v = [2\alpha E/(M + wr)]^{1/2}, \quad (3)$$

where E and M are the kinetic energy and the mass of the ejecta, respectively, and α is the ratio of kinetic to total energy (typically 1/2). For the parameters of SN 1995G, this gives $M_{\rm ej}/{\rm M_\odot} = 3E_{51}$, so if $E \simeq 10^{51}$ erg, $M_{\rm ej} \simeq 3\,{\rm M_\odot}$.

Since it is not clear which phase of the interaction was observed in SN 1995G, the mass of the ejecta can be estimated from the above considerations to be in the range $3-9\,{\rm M_\odot}$, provided that $\psi = 1$ and $E = 10^{51}$ erg. Including the mass of the neutron star remnant, we obtain a pre-SN mass between 5 to $11\,{\rm M_\odot}$, which corresponds to zero-age main-sequence masses around $15-20\,{\rm M_\odot}$ if a new empirical formulation of the mass-loss rate and a diffusive approach of turbulent mixing is adopted (Salasnich, Bressan & Chiosi 1999). We stress that the values of the mass loss are very sensitive to metallicity, and that the estimates of $M_{\rm ej}$ are strongly dependent on the value of the explosion energy. The uncertainties on the progenitor mass are therefore very large, meaning that it could be significantly lower.

As for the Hα luminosity, this is a constant factor of 6 smaller in SN 1995G than in SN 1988Z. However, the width of the intermediate component of Hα is about 4–5 times smaller (2000 versus $9000\,{\rm km\,s^{-1}}$), so if the wind is clumpy as in SN 1988Z, but the density is higher in SN 1995G ($\dot{M}$ was higher), this may be a natural result.

We note also that the small inferred mass of the precursor of SN 1988Z ($8-10\,{\rm M_\odot}$) is a consequence of the assumptions $E = 10^{51}$ erg and $\psi = 1$. If a higher value of the kinetic energy is used for SN 1988Z, as may be suggested in Aretxaga et al. (1999), a larger ejecta mass is obtained. On the other hand, decreasing ψ leads to a higher wind density and mass-loss rate (and to a larger mass lost in the wind), but it also leads to a smaller ejecta mass through equation (1). Whether this leads to a significantly different estimate of the mass of the progenitor is not clear, however, as this depends on the duration of the strong RSG wind episode.

6 CONCLUSIONS

This paper presents the photometric and spectroscopic observations of SN 1995G obtained at ESO La Silla, Lick and Asiago, over a period of more than 4 years after the discovery.

The broad-band and bolometric light curves are flatter than those expected from radioactive decay. The luminosity peak and evolution are very similar to those of the well-studied SN 1988Z. This implies the presence of an additional source of energy, most likely the interaction of the ejecta with a dense CSM.

The line profiles show evidence of different components. The strongest line, Hα, shows relatively narrow P Cygni profiles with minima displaced by $700-800\,{\rm km\,s^{-1}}$ superimposed on an intermediate-width emission FWHM $\approx 2000\,{\rm km\,s^{-1}}$ and on a broader component having FWHM $\approx 4000\,{\rm km\,s^{-1}}$. The widths of these emission lines decrease with time. At 942 days after maximum the Hα emission has a boxy shape with FWZI $= 2500\,{\rm km\,s^{-1}}$, suggesting that most of the expanding shell has

been swept away and that the optical depth of the material is low. The emission lines of SN 1995G were narrower than in SN 1988Z, indicating slower expansion velocities of the ejecta.

The detection of strong He lines between about 200 and 600 days after the discovery indicates the presence of non-thermal effects. Simple considerations about the density of the slowly expanding material indicate densities $n_{\rm H} \gg 10 \times 10^8\,{\rm cm}^{-3}$, in agreement with the absence of forbidden lines.

On the hypothesis that the additional source of luminosity of SN 1995G is the conversion to radiation of the kinetic energy of the ejecta due to interaction with a precursor wind, we estimate the mass of the ejecta and the mass loss. We obtain $M_{\rm ej} \simeq 3$–$9\,{\rm M}_\odot$ and $\dot{M} = 0.002\,{\rm M}_\odot\,{\rm yr}^{-1}$, respectively, provided that the conversion efficiency is $\psi = 1$ and the explosion energy is $E = 10^{51}$ erg.

ACKNOWLEDGMENTS

We acknowledge support from the Italian Ministry for University and Scientific and Technological Research (MURST) through grant Cofin MM02905817. A. V. Filippenko is grateful for a Guggenheim Fellowship and for NSF grant AST–9987438. This paper was based on observations collected at ESO – La Silla (Chile), Asiago (Italy) and Lick (USA).

REFERENCES

Almog Y., Netzer H., 1989, MNRAS, 238, 57
Aretxaga I. et al., 1999, MNRAS, 309, 343
Baldwin J. A., Stone R. P. S., 1984, MNRAS, 206, 241
Benetti S., Bouchet P., Schwarz H., 1995, IAU Circ. 6170
Benetti S., Cappellaro E., Danziger I. J., Turatto M., Patat F., Della Valle M., 1998, MNRAS, 294, 448
Benetti S., Turatto M., Cappellaro E., Danziger I. J., Mazzali P. A., 1999, MNRAS, 305, 811
Benetti S. et al., 2001, MNRAS, 322, 361
Cappellaro E., 1999, IAU Circ. 7304
Cappellaro E., Turatto M., Mazzali P. M., 1999, IAU Circ. 7091
Carter B. S., Meadows V. S., 1995, MNRAS, 276, 734
Catchpole R. M. et al., 1987, MNRAS, 229, 15P
Catchpole R. M. et al., 1988, MNRAS, 231, 75P
Catchpole R. M. et al., 1989, MNRAS, 237, 55P
Chugai N. N., Danziger I. J., 1994, MNRAS, 268, 173
de Vaucouleurs G., de Vaucouleurs A., Corwin H. G., Buta R. J., Paturel G., Fouqué P., 1991, Third Reference Catalogue of Bright Galaxies. Springer-Verlag, Berlin, Heidelberg, New York (RC3)
Dopita M. A., Cohen M., Schwartz R. D., Evans R., 1984, ApJ, 284, 69
Evans R. O., Shobbrook J., Beaman S., Cass P., 1995, IAU Circ. 6138
Fassia A. et al., 2000, MNRAS, 318, 1093
Fassia A. et al., 2001, MNRAS, 325, 907
Filippenko A. V., 1991, in Danziger I. J., Kjar K., eds, SN 1987A and Other Supernovae. ESO, Garching, p. 343
Filippenko A. V., 1997, ARA&A, 35, 309
Filippenko A. V., Schlegel D., 1995, IAU Circ. 6139
Filippenko A. V., Leonard D. C., Riess A. G., 1999, IAU Circ. 7091
Fox D. W. et al., 2000, MNRAS, 319, 1154
Fransson C., 1984, A&A, 132, 115
Fransson C. et al., 2001, ApJ, submitted (astro-ph 0108149)
Germany L. et al., 2000, ApJ, 533, 320
Grandi S. A., 1980, ApJ, 238, 10
Hamuy M., Walker A. R., Suntzeff N. B., Gigoux P., Heathcote S. R., Phillips M. M., 1992, PASP, 104, 533
Hamuy M., Suntzeff N. B., Heathcote S. R., Walker A. R., Gigoux P., Phillips M. M., 1994, PASP, 106, 566
Huchra J., Latham D. W., Da Costa L. N., Pellegrini P. S., Willmer C. N. A., 1993, AJ, 105, 1637
Hunt L. K., Mannucci F., Testi L., Migliorini S., Stanga R. M., Baffa C., Lisi F., Vanzi L., 1998, AJ, 115, 2594
Landolt A. U., 1992, AJ, 104, 340
McNaught R. H., Cass C. P., 1995, IAU Circ. 6140
Mihalas D., 1978, Stellar Atmospheres, 2nd ed. Freeman, San Francisco
Patat F., Barbon R., Cappellaro E., Turatto M., 1994, A&A, 282, 731
Persson S. E., Murphy D. C., Krzeminsky W., Roth M., Rieke M. J., 1998, AJ, 116, 2475
Proga D., Mikolajewska J., Kenyon S. J., 1994, MNRAS, 268, 228
Rybicki G. R., Hummer D. G., 1978, ApJ, 219, 654
Salamanca I., Cid-Fernandes R., Tenorio-Tagle G., Telles E., Terlevich R. J., Munoz-Tunon C., 1998, MNRAS, 300, L17
Salamanca I., Terlevich R. J., Tenorio-Tagle G., 2002, MNRAS, 380, 884
Salasnich B., Bressan A., Chiosi C., 1999, A&A, 342, 131
Schlegel D. J., Finkbeiner D. P., Davis M., 1998, ApJ, 500, 525
Schlegel E. M., 1990, MNRAS, 244, 269
Sollerman J., Cumming R. J., Lundqvist P., 1998, ApJ, 493, 933
Stathakis R. A., Sadler E. M., 1991, MNRAS, 250, 786
Stone R. P. S., Baldwin J. A., 1983, MNRAS, 204, 237
Terlevich R., Tenorio-Tagle G., Franco J., Melnick J., 1992, MNRAS, 255, 713
Turatto M., Cappellaro E., Danziger I. J., Benetti S., Gouiffes C., Della Valle M., 1993, MNRAS, 262, 128
Turatto M. et al., 1998, ApJ, 498, 129
Turatto M. et al., 2000, ApJ, 534, 57

This paper has been typeset from a TEX/LATEX file prepared by the author.